




Article

Investigation of the Adsorption Process of Biochar Açai (*Euterpe oleracea* Mart.) Seeds Produced by Pyrolysis

Lauro Henrique Hamoy Guerreiro¹, Ana Cláudia Fonseca Baia¹, Fernanda Paula da Costa Assunção², Gabriel de Oliveira Rodrigues³, Rafael Lopes e Oliveira³, Sergio Duvoisin Junior³, Anderson Mathias Pereira⁴, Erika Milene Pinto de Sousa⁵, Nélio Teixeira Machado⁶ , Douglas Alberto Rocha de Castro⁷  and Marcelo Costa Santos^{1,*} 

- ¹ Graduate Program of Chemical Engineering, Campus Profissional-UFFPA, Federal University of Pará, Rua Augusto Corrêa N°1, Belém 66075-110, Brazil
 - ² Institute of Technology, Federal University of Pará, Rua Augusto Corrêa N°1, Belém 66075-110, Brazil
 - ³ Faculty of Chemical Engineering, State University of Amazonas-UEA, Avenida Darcy Vargas N°1200, Manaus 69050-020, Brazil
 - ⁴ Faculty of Agricultural Sciences, Federal University of Amazonas, Av. Gen. Rodrigo Octávio N°6200, Manaus 69080-900, Brazil
 - ⁵ Study Group on Biomass Processing, Federal Rural University of the Amazon, Campus Capanema, Avenida Barão de Capanema, SN, Bairro Caixa D'água, Capanema 68700-665, Brazil
 - ⁶ Faculty of Sanitary and Environmental Engineering, Applied Chemistry Research Group, Campus Profissional-UFFPA, Universidade Federal do Pará, Rua Corrêa N°1, Belém 66075-900, Brazil
 - ⁷ Cursos de Engenharia Química, Mecânica e Elétrica, Lutheran University Center of Manaus—CEULM/ULBRA, Avenida Carlos Drummond de Andrade N°1460, Manaus 69077-730, Brazil
- * Correspondence: marcelo.santos@ufpa.edu.br; Tel.: +55-(91)-98948-6741



Citation: Guerreiro, L.H.H.; Baia, A.C.F.; Assunção, F.P.d.C.; Rodrigues, G.d.O.; e Oliveira, R.L.; Junior, S.D.; Pereira, A.M.; de Sousa, E.M.P.; Machado, N.T.; de Castro, D.A.R.; et al. Investigation of the Adsorption Process of Biochar Açai (*Euterpe oleracea* Mart.) Seeds Produced by Pyrolysis. *Energies* **2022**, *15*, 6234. <https://doi.org/10.3390/en15176234>

Academic Editor: Javier Fermoso

Received: 26 July 2022

Accepted: 23 August 2022

Published: 26 August 2022

Publisher's Note: MDPI stays neutral with regard to jurisdictional claims in published maps and institutional affiliations.



Copyright: © 2022 by the authors. Licensee MDPI, Basel, Switzerland. This article is an open access article distributed under the terms and conditions of the Creative Commons Attribution (CC BY) license (<https://creativecommons.org/licenses/by/4.0/>).

Abstract: This work aims to investigate the influence of temperature and chemical impregnation in the textural and morphological composition of the bio-adsorbent of bio-adsorption via thermal cracking of the seeds of açai. The experiments were carried out at 400 °C and 450 °C using a pilot scale reactor. The efficiency of the organic process was calculated in terms of liquid and solid products selected with a chemical impregnation process with NaOH, mainly with the liquid that had a greater product conversion. The elementary samples of the solid products occur with the occurrence of carbonization with an increase in the temperature of the process and the presence of impregnation. The textural and morphological characterization occurred with an analysis of FT-IR, SEM/EDS, XRF, and B.E.T. The in-phase product was developed through the creation of açai seed in nature and impregnated with NaOH solution (2 M) at temperatures of 400 °C and 450 °C. The adsorption kinetics of acetic acid were investigated at 5, 10, 15, 20, 60, 120, and 180 s. The adsorption is higher at 450 °C and with the chemical impregnation of NaOH since the experiments were able to remove an amount of 317.51 mg acid/g adsorbent acetic acid. All the models analyzed fit the experiments, both for the kinetic models (pseudo-first order and pseudo-second order) and for the equilibrium models (Langmuir and Freundlich).

Keywords: açai (*Euterpe oleracea*); lignocellulosic biomass; biochar; adsorption

1. Introduction

Severe climate problems and energy crises have become the main factors contributing to the use of biomass materials as an alternative source of energy and fuels [1,2]. The rational use of available energy and plant biomass residues are alternatives to minimize these issues. In this scenario, agro-industrial residues constitute renewable natural reserves, available in large quantities in nature and represent an important source of raw materials that can be used in chemical and biotechnological processes [3,4]. Terrestrial biomass, extensively considered sustainable, is CO₂ neutral and is the most abundant carbonaceous

feedstock, developed in recent decades as an alternative source of fossil feedstocks for the production of renewable fuels [5,6].

The use of biomass generated from agro-industrial residues, such as açai seed (generated by pulping the fruit), serves as a raw material for the development of high value-added products, one of which is biochar, commonly obtained by pyrolysis [7,8]. In recent years, the literature reports the application of biochar as a bio-adsorbent to selectively remove organic and inorganic compounds, as well as heavy metals, that is, the adsorption/sorption of contaminants [9].

Biochar has been applied as an adsorbent due to its ability to selectively remove and/or absorb polar and non-polar organic compounds, including acetic acid [9]. The degradation of biosolids by pyrolysis produces biochar and reduces the number of pathogens, as well as the availability of contaminants, which improves the quality of the residues and allows its application in the soil, both as an additive and as a soil conditioner [10]. The production of biochar with appropriate properties will also determine its sorption capacity towards various contaminants. In the literature, it has been demonstrated many times that biomass-derived biochar strongly absorbs hydrocarbons, pigments, phenols, pesticides, polycyclic aromatic hydrocarbons (PAHs), antibiotics, and some inorganic metal ions [11,12].

Adsorption is one of the most common phenomena in nature, it plays a critical role in fields involved with surface and interface processes. Adsorption is crucial for chemical and biological processes involving gas–solid and/or solid–liquid interfaces such as molecular detection, heterogeneous catalysis, material synthesis, and electrochemistry [13]. The adsorption process is economically viable and produces a high-quality product. The first step towards an efficient adsorption process is choosing an adsorbent with high selectivity, high capacity, and long life. This must also be available in large quantities at a low cost [14].

Biomass is composed of three major components: cellulose, hemicellulose, and lignin. Structural and chemical differences lead to different chemical reactivity, meaning that the relative composition of cellulose, hemicellulose, and lignin in the biomass is a crucial factor for the processes. Cellulose is a linear polymer of ether-linked anhydro glucopyranose units. Hemicellulose is a polymer composed of sugar units. Lignin is a complex, cross-linked three-dimensional polymer formed with phenylpropane units [15]. Figure 1 represents the structure of lignocellulosic biomass.

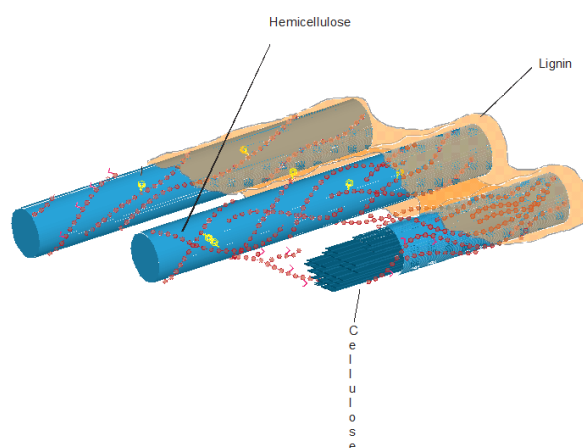


Figure 1. Composition of lignocellulosic biomass [16].

Lignocellulosic biomasses still have ash and moisture in their composition. The ash corresponds to inorganic constituents that mainly include SiO_2 , CaO , K_2O , P_2O_5 , Al_2O_3 , MgO , Fe_2O_3 , SO_2 , Na_2O , and TiO_2 , as determined by EDX [17]. The generated biomass is considered to have environmental liabilities, in which one of the treatment biases is the pyrolysis process, that is, the combustion of biomass to generate products in the form of gases, liquids, and solids. The conversion of biomass to bioenergy using pyrolysis technology has received a lot of attention as it is a sustainable and ecological approach

to producing energy. Pyrolysis is a thermochemical process that transforms biomass into biochar, bio-oil, and gas. The co-production of bioenergy sources with biochar makes the pyrolysis technique more sustainable and ecological than producing biochar alone [18]. In the process, most of the biomass ends up as a liquid, bio-oil, or solid biochar [16].

Açaí seeds, a lignocellulosic material rich in fiber oil, whose centesimal composition reported in the literature consists of lipids between 1.65 and 3.56% (*w/w*), total fibers between 29.69 and 62.75% (*w/w*), hemicellulose between 39.83 and 40.29% (*w/w*), lignin between 4.00 and 8.93% (*w/w*), moisture between 10.15 and 39.39% (*w/w*), protein between 5.02 and 7.85% (*w/w*), 0.83% (*w/w*) of fixed carbon, and 7.82% (*w/w*) of volatile material, approximately [8]. Figure 2 represents the parts that make up the açaí fruit.

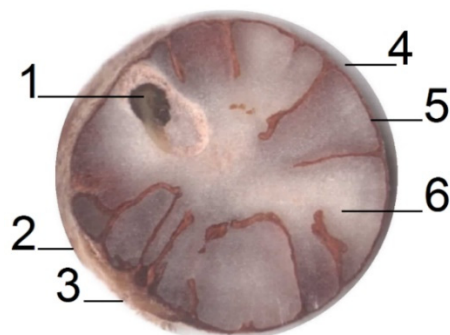


Figure 2. Anatomy of the açaí fruit (cross-section): (1) Embryo, (2) Endocarp, (3) Scar, (4) Pulp, (5) Pericarp + Tegument, and (6) Mesocarp [19].

Due to the environmental damage caused by the incorrect disposal of the açaí seed, alternative uses were explored, such as handicrafts and the use of renewable energy [20]. Thus, the production of biochar also appears as an alternative to the irregular disposal of these residues [21]. Biomass pyrolysis, as one of the most basic components of biomass, has been the subject of extensive studies in the past. Previous studies on hemicellulose pyrolysis mechanisms focused primarily on experimental studies to explore the rate of oil, gases, and coke under different conditions. Biomass can be transformed through thermochemical processing, such as pyrolysis into liquid bio-oil, which can be stored and used for different applications. Biomass contains varying amounts of cellulose, hemicellulose, lignin, and a small number of extractives. The proportion of the three components in biomass, which is closely related to biomass conversion, differs greatly with the source of the biomass, so the study of the pyrolysis mechanism of the biomass components is essential [22,23].

Castro et al. [9] are developing the use of biomass açaí seed, an environmental liability, for the production of bio-oil, activated carbon, and bio-gas via thermal and thermocatalytic pyrolysis, using 2 molar NaOH as a catalyst. The conversion of biomass to bioenergy using this technology has received increasing attention as it is a sustainable and environmentally friendly approach to energy production [18–24]. The co-production of bioenergy sources with biochar makes the technique more sustainable and ecologically correct than the isolated production of biochar [18]. The specific properties of biochar that qualify it as a potential adsorbent for the removal of pollutants from aqueous solutions include: a high specific surface area, a porous structure, and a surface rich in functional groups and mineral components. As an adsorbent, biochar has a porous structure, similar to activated carbon, the most commonly used adsorbent, and also the most efficient, in the removal of various pollutants from water worldwide [25,26].

Studies such as the one by Sato et al. [27], which produced biochar from açaí seeds via a pyrolysis process for application in the soil, state that after applying the biochar for 270 days, it was verified that there was an improvement in the physical composition of the soil, with greater absorption of nutrients such as potassium and magnesium, and reducing the presence of aluminum, justifying the use of biochar as an adsorbent for nutrient uptake and soil correction.

Adsorption is a mass transfer operation, which studies the ability of certain solids to concentrate on their surface certain substances existing in liquid or gaseous fluids, enabling the separation of the components of these fluids. Since the adsorbed components are concentrated on the external surface, the greater this external surface per unit of solid mass, the more favorable the adsorption will be. Therefore, generally, adsorbents are solids with porous particles. The species that accumulates at the material interface is usually called adsorbate, and the solid surface on which the adsorbate accumulates is called the adsorbent. [28,29]. The adsorption separation processes are based on three distinct mechanisms: the steric mechanism, the equilibrium mechanisms, and the kinetic mechanism. For the steric mechanism, the pores of the adsorbent material have characteristic dimensions, which allow certain molecules to enter, excluding the others. For equilibrium mechanisms, there are the abilities of different solids to accommodate different species of adsorbates, which are preferentially adsorbed into other compounds. The kinetic mechanism is based on the different diffusivities of the different species in the adsorbent pores [29,30]. In recent years, several studies have been published on the application of adsorption in the removal of impurities from vegetable oils, but we found little information when it comes to the treatment of biofuels using adsorption [31].

In this way, aiming at a solution for the application of these residues generated by the agroindustry and to verify the potential use of biochar in the acidity correction of biofuels generated from renewable materials, the objective of this work is to use two types of adsorbent biochar, the *in natura* and biochar impregnated at 400 °C and 450 °C, produced from açai seeds, for the analysis of their potential for adsorption of acetic acid (CH_3OOH) in solution. A part of the pits that gave rise to the biochar was impregnated with $2 \text{ mol}\cdot\text{L}^{-1}$ of NaOH, and the other part was kept *in natura*. In this way, the feasibility of using a bio-adsorbent from the solid residue of a regional fruit that is highly consumed in the Amazon, the açai, was tested.

2. Materials and Methods

2.1. Methodology

Figure 3 outlines the methodology as a rational scheme of ideas, methods, and procedures to produce the bio-adsorbent. The chemically activated and the *in natura* adsorbents were applied to uptake acetic acid from aqueous solutions. Initially, the açai seeds were collected. Afterwards, they were submitted to pretreatments of drying, grinding, and sieving. The pyrolysis process was carried out in a closed system, i.e., the pilot scale, as described elsewhere [8]. The biochar was characterized by SEM/EDX, FRX, and B.E.T. The biochar was obtained by processing the açai seeds in nature and chemical activation at temperatures of 400 °C and 450 °C. The adsorption of acetic acid (CH_3COOH) on biochar was investigated by analyzing the adsorption kinetics, adsorption equilibrium, and sorption equilibrium capacity at the laboratory scale.

2.2. Drying

After collecting the raw material, 750 kg of seeds (wet) were weighed and separated into five loads of 150 kg to be subjected to the drying process, which was carried out in a pilot thermal oven with air recirculation and analog SOC temperature control (FABBE. Ltd. a, MOD. 170) at 110 °C for a period of 24 h in the Laboratory of Thermal Separations (THERMITEK/FEQ/ITEC/UFPA) in order to reduce the moisture content of açai seeds.

2.3. Comminution

After the drying process, the Comminution Process was carried out for two loads of seeds with the aid of a knife mill model TRAPP TRF 600. For the first load (50 kg) a comminution sieve with an opening diameter of 0.8 mm was used, and for the remaining load, a 5 mm sieve was used at the Materials Plant of the Faculty of Chemical Engineering (USIMAT/FEQ/ITEC/UFPA). Soon after, the sieving was carried out using a 0.6 mm sieve in order to remove excess fibers from the açai seed.

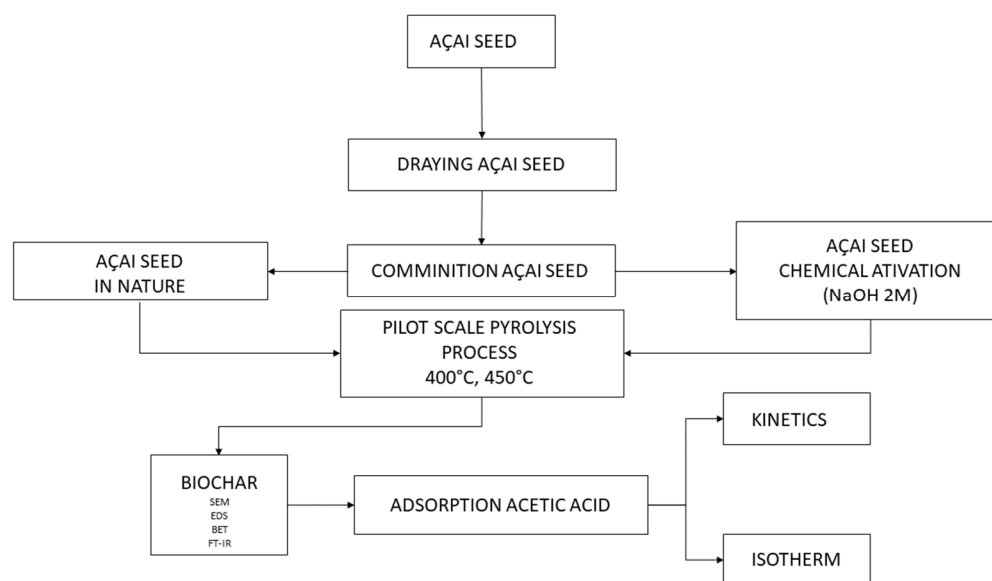


Figure 3. Process diagram of adsorption of acetic acid (Author).

2.4. Chemical Activation

The chemical activation processes in the açai seeds were carried out in amounts of masses corresponding to the pilot scale of the pyrolysis experiments performed. Given this aspect, for each batch, $2.0 \text{ mol}\cdot\text{L}^{-1}$ of sodium hydroxide (NaOH) was impregnated with an aqueous solution, and 32 kg of the comminuted sample was used for the impregnation process. The proportion (w/v) of seeds in the solution used was (1:2), respectively; that is, the volume of the NaOH solution was twice the mass of seeds. Additionally, for the pilot scale experiments, commercial caustic soda was used in scales (UNIPAR CARBOCLORO; Purity: 95.5%).

The pilot impregnation process (32 kg of comminuted sample and 64 L of NaOH solution) was carried out at the Thermal Separations Laboratory (THERMITEK/FEQ/ITEC/UFPA) with the aid of a pilot mechanical stirrer with a marine propeller impeller and a capacity of 110 L, at room temperature and atmospheric pressure, and an agitation speed of 1000 RPM.

After the predetermined period of time for the impregnations of the açai seeds, the phases were separated through the Simple Filtration Process carried out with the aid of a filter funnel and a porous filter medium (Qualitative Filter Paper 24.0 Ø; Brand: J. PROLAB) with the following technical specifications: Weight: $80 \text{ g}/\text{m}^2$; Thickness: $205 \mu\text{m}$; Gray: 0.5%; Pores: $14 \mu\text{m}$, where the excess of the aqueous phase was removed. Then, they were subjected to a new drying process at $100 \text{ }^\circ\text{C} \pm 5 \text{ }^\circ\text{C}$ for a period of 24 h to retain the remaining moisture and the solid phase for subsequent performance of the Pyrolysis Process.

2.5. Physicochemical Characterization of Açai Seeds

The characterization of the açai seeds in nature was carried out after the drying process. Therefore, immediate analyses were carried out (Moisture, Ash, Volatiles, and Fixed Carbon) from the sampling of the previously dried seeds. The procedures used were performed according to ASTM D 3173-87, ASTM D 3174-04, and ASTM D 3175-04, respectively. These analyses were performed at the Thermal Separations Laboratory (THERMITEK/FEQ/ITEC/UFPA).

2.6. Morphological, Crystalline, and Textural Characterization of Biochars

The morphological, crystalline, and textural characterization of the biochars obtained by the pyrolysis processing of açai seeds at 400 and 450 °C, using a reactor pilot scale, was performed by SEM, EDX, and FRX (the equipment and procedures were described elsewhere) as well as by B.E.T. [8].

2.7. Adsorption of CH_3COOH

The adsorption kinetics of acetic acid on biochars produced by the thermal pyrolysis of açai seeds at 400 °C and 450 °C, on a pilot scale, with the product in nature and chemically activated with NaOH, was systematically investigated. The adsorption of CH_3COOH can be investigated by determining the initial concentration of the acetic acid solution and the concentrations of CH_3COOH in aqueous solutions over time until the time reaches equilibrium. To obtain the adsorption isotherms, 10 mL of the solutions were used with a concentration of 1% *v/v* and a mass of approximately 0.1 g of adsorbent, under mechanical agitation, for a period of contact. After defined times of 0, 5, 10, 15, 20, 30, 60, 90, 120, and 180 s, they were filtered and, via titration with NaOH solution, the acid value of the filtered adsorbate was verified.

2.8. Adsorption Equilibrium, Adsorption Kinetics, and Isotherms

2.8.1. Adsorption Equilibrium

Adsorption equilibrium is generally an essential requirement for obtaining relevant information about the design and analysis of an adsorption separation process. When a given amount of a solid, commonly called an adsorbent or adsorbent, comes into contact with a given volume of a liquid containing an adsorbable solute, this is called an adsorbate or adsorbate. Adsorption occurs until equilibrium is reached [32].

The adsorption equilibrium is important information for understanding the adsorption process. No matter how many of the components are present in the system, the adsorption balance of pure components is essential to understanding how the components can be accommodated by the solid adsorbent. This information can be used to study the adsorption kinetics of a single component, as well as the adsorption equilibrium and adsorption kinetics of multi-component systems [33].

The main factors that influence the adsorption equilibrium are the porous structure of the solid, its heterogeneity, and its surface chemical properties. The adsorption phenomenon also depends on the differences between the chemical properties of the solvent and adsorbate [34].

2.8.2. Adsorption Kinetics

The kinetic aspect provides information about the rate of adsorption. This rate depends on the size and structure of the adsorbate molecule, the nature and porosity of the adsorbent, and the experimental system. It also depends on the transport of the adsorbate from the solution to the surface of the adsorbent, and this step can be controlled by the diffusion process [13].

Kinetic models involve the relationship of the adsorbate concentration with the stirring time. The concentration of the adsorbate in solution decreases with time until reaching a constant value. At this point, the amount of adsorbate being adsorbed by the adsorbent is in dynamic equilibrium with the amount being desorbed. The time required to reach this stage is called the equilibrium time, and the amount of adsorbate retained in this time reflects the adsorption capacity at equilibrium under established operating conditions. The mass of adsorbate retained per unit mass of adsorbent matter (q_t) at time (t) ($\text{mg}\cdot\text{g}^{-1}$), obtained in batch reactors, is calculated using a mass balance according to Equation (1) [13].

$$q_t = \frac{(C_0 - C_t) \times V}{m} \quad (1)$$

2.8.3. Isotherms

A simple analysis of the adsorption kinetics, performed by the pseudo-first-order Lagergren equation, based on the solids' capacity, is given by Equation (2). It assumes that the rate of adsorbate removal with time is directly proportional to the difference in saturation concentration and to the number of active sites in the solid. The adsorption

rate of this model is determined by a pseudo-first-order expression for adsorption in a liquid/solid system based on the capacity of the solid [13].

$$\frac{dq_t}{dt} = K_1 (q_e - q_t) \quad (2)$$

Performing the integration and applying the boundary conditions $q_t = 0, t = 0$; when $q_t = q_t, t = t$ has the linearized form as presented in Equation (3).

$$\log (q_e - q_t) = \log q_e - \frac{K_1}{2.303} \times t \quad (3)$$

The pseudo-second-order model is based on the adsorption capacity of the solid phase. The model considers that the reaction rate is dependent on the amount of solute adsorbed on the surface of the adsorbent and on the amount adsorbed at equilibrium. Unlike the Lagergren model, the Ho and Mckay model probably predicts kinetic behavior throughout the adsorption process and is consistent with a mechanism in which chemical adsorption is the determining step of the process [10]. Based on equilibrium adsorption, the pseudo-second-order model can be expressed in the form of Equation (4) [13].

$$\frac{Dq_t}{dt} = K_2 \times (q_e - q_t)^2 \quad (4)$$

Applying the integration, we have the model presented in Equation (5).

$$\frac{1}{q_t} = \frac{1}{K_2 \times q_e} + \frac{1}{q_e} \times t \quad (5)$$

3. Results and Discussion

3.1. Physical Characterization of Açai Seeds

The physical characterization of the açai seeds was carried out by determining the moisture content, volatile content, ash content, fixed carbon content, and higher calorific value after drying in an oven at 105 °C. Table 1 shows the values available in the literature for the palm tree *Euterpe oleracea* Mart found by Rambo [35] and Seye [36].

Table 1. Physical characterization of açai seeds.

Analysis	Açai Seeds	Rambo [35]	Seye [36]
Moisture (%)	12.45	13.27	6.13
Volatiles Content (%)	85.98	80.77	80.35
Ash Content (%)	0.42	0.69	1.15
Fixed Carbon Content (%)	1.15	18.50	18.50
Higher Calorific Power (MJ/mg)	13.81	18.60	16.36

From the results shown in Table 1, we can assess whether the values of the analyses are in line with the results obtained in the literature. As it turns out, the humidity is close to the value obtained by Rambo [35] with 12.45%; however, there is a significant increase when compared to Seye [36] of 53.51%. This difference can be explained due to the authors using different species of the fruit and also by the way these fruits were stored after pulping. The content of volatile materials is close to those found in the literature and studied by Rambo [35] and Seye [36]. In view of the results analyzed above, the humidity value becomes significant for the thermal cracking process, increasing the heating time that favors the production of bio-oil and activated carbon, which is under study. However, the values obtained for the other parameters evaluated favor the pyrolysis process, with regard to the generation of solid, liquid, and gaseous products, according to studies by Machado [37].

3.2. SEM and EDX Açai Seeds Analysis

SEM analysis was performed on açai seeds in nature and açai seeds chemically activated with sodium hydroxide, with the objective of verifying the morphology of the natural seed after the process of chemical impregnation and modification of the surface structure of the seed. Figure 4 shows the SEM performed on the samples mentioned above.

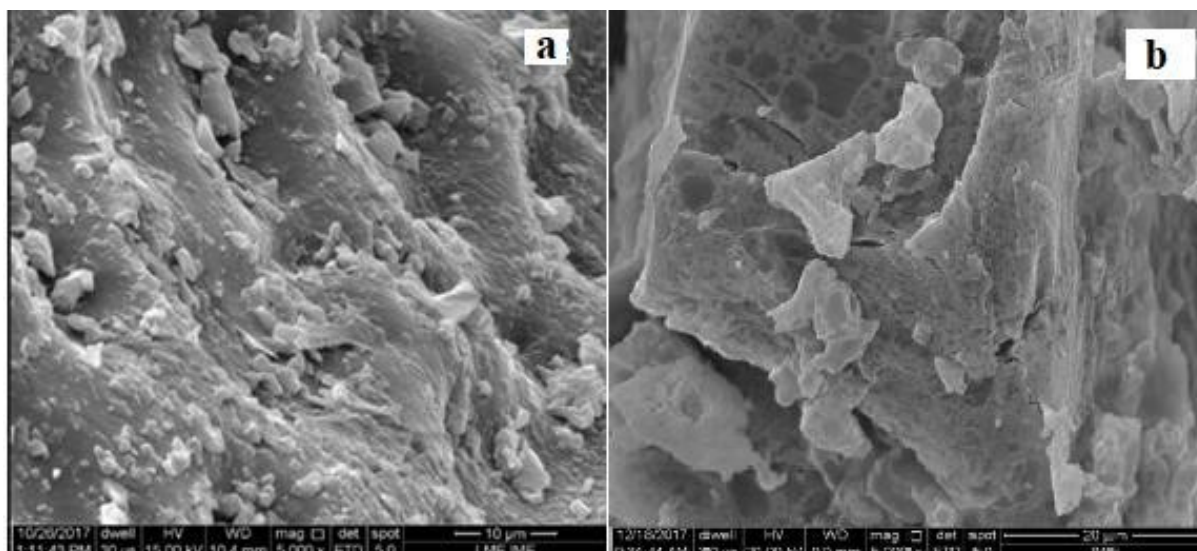


Figure 4. (a) Microscopy of açai seed in nature at 5000× magnification. (b) Microscopy of açai seed impregnated with NaOH at 5000× magnification.

Analyzing the SEM of açai seeds in nature in comparison with that of the chemically impregnated seeds shows the change in the morphology of the surface structure of the samples. It is noticeable in the first image, an amorphous and homogeneous shape with irregular shapes in its structure, also showing a concave and closed structure, without the presence of sites in its structure. This is different when analyzing the SEM of the sample with impregnation in which we verify a change in the morphological structure, losing the concave and closed structure; however, it is more compacted, presenting more regular shapes. According to what was studied by Castro [8] and Leão [38], this structural modification attributed to the influence of the treatment with sodium hydroxide contributed to the reduction in hemicellulose and lignin in the morphological structure of the açai seeds.

The semi-quantitative chemical analysis by EDX of the açai seed in nature and impregnated registered the three main elements Carbon (C), Oxygen (O), and Sodium (Na). Table 2 shows the percentages of elements present.

Table 2. EDX analysis of açai seeds in nature and impregnated.

Chemical Elements	In Nature		Impregnated	
	Mass (w%)	Atomic Mass (w%)	Mass (w%)	Atomic Mass (w%)
C	79.28	83.64	55.67	64.05
O	20.71	16,36	35.29	30.51
Na	-	-	9.04	5.44
Total (%)	100.00	100.00	100.00	100.00

Analyzing the results in Table 2, they show a significant difference in carbon in the structure of the in natura compared to the impregnated one, with a decrease occurring after the chemical attack on the açai seed, which can also be explained by the removal of lignins and hemicelluloses from the açai seed structure. The addition of Oxygen to the

impregnated structure impairs the thermal pyrolysis process, as this will cause instability in the burning process of the material inside the reactor. The presence of sodium hydroxide, as was also seen in the SEM, is due to the chemical impregnation process; the NaOH is in the surface structure of the açai seed.

In comparison to the analyses carried out by Cordeiro [17], there is a higher percentage in the present work of the presence of Carbon, with an increase of almost 30%, and with a percentage of Oxygen below, comparing the açai seed in nature.

3.3. SEM and EDX Biochar Analysis

With the SEM analysis, it was possible to verify the quality of the charcoal produced via thermal cracking at temperatures of 400 °C and 450 °C of the açai seed in nature and chemically impregnated. Figures 5 and 6 represent the micrographs of the in natura and impregnated samples, respectively, which identify the morphological changes of the original product of solid particulates in order to evaluate variations in temperature and chemical treatment with NaOH.

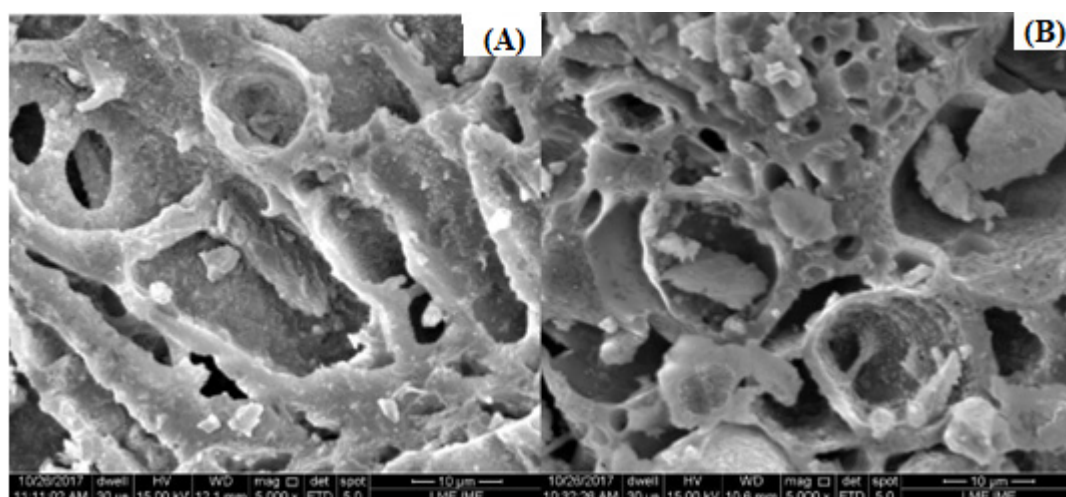


Figure 5. (A) Micrographs of biochar in nature obtained at 400 °C. (B) Micrographs of biochar in nature obtained at 450 °C.

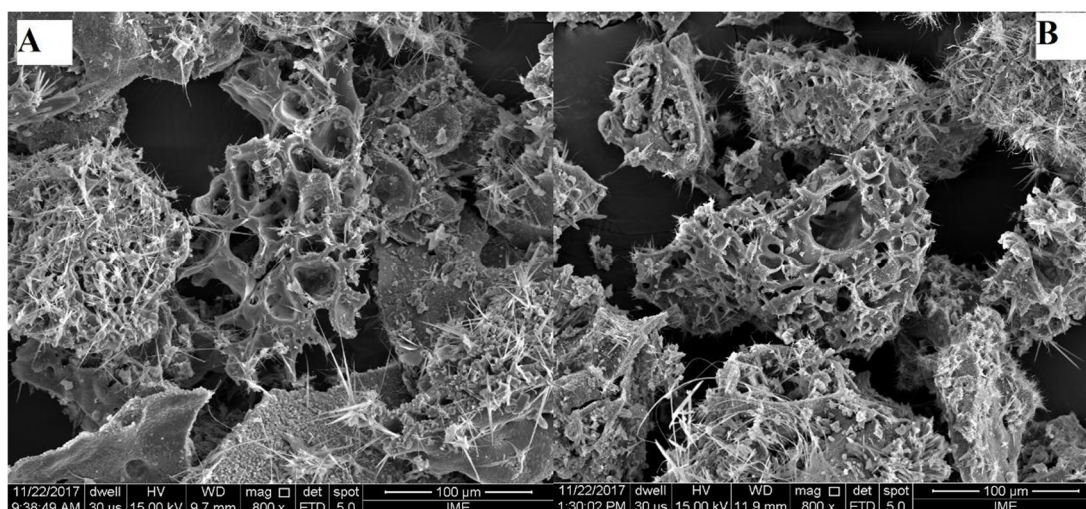


Figure 6. Micrographs of biochar impregnated obtained at 400 °C (A) and 450 °C (B).

Analyzing the results of the SEM image analysis for the in natura charcoals for the test temperatures of 400 °C and 450 °C, image (A) shows a difference in the SEM of the

in natura açai seed before the pyrolysis process, and the charcoal presents more defined pores in its morphology. In image (B), we can see the same difference after performing the pyrolysis process at 450 °C; this can be seen because the lignocellulosic raw material has a closed surface morphology, as seen in Figure 4.

In Figure 5, comparing the biochar obtained at different temperatures, it is observed that visually there is no significant change. Such changes will be able to be verified in real adsorption experiments, mainly in the equilibrium kinetics. The micrograph shows surface structures consisting of some open cells and others partially closed or totally closed for the biochar obtained at a temperature of 400 °C. The surface structure at 450 °C did not show different changes to the previous temperature.

Table 3 shows the EDX analysis. It is verified that, with increasing process temperature, there is an increase in the amount of carbon, and oxygen decreases. The compounds identified at the biochar analysis point are in agreement with those seen in organic materials. The increase in temperature from 400 °C to 450 °C shows that the biochar undergoes carbonization.

Table 3. EDX analysis of biochar in nature.

Chemical Elements	Biochar 400 °C		Biochar 450 °C	
	Mass (w%)	Atomic Mass (%)	Mass (w%)	Atomic Mass (%)
C	82.08	88.16	89.98	93.56
O	9.96	9.96	6.95	5.42
K	5.33	1.76	2.45	0.78
Al	0.24	0.11	-	-
S	-	-	0.61	0.24
Total (%)	100	100	100	100

Figure 6 shows the image analysis for the raw material that underwent chemical impregnation after having gone through the pyrolysis process at 400 °C and 450 °C. In the SEM, the presence of crystals composed of sodium molecules is observed, which remained in the biochar after the process of pyrolysis. Comparing the biochar produced in nature and the chemically impregnated one, a greater definition of the pores can be seen for the biochar that has undergone chemical treatment, presenting, for the most part, open pores with a larger diameter. The biochar presented a better structure for adsorption of the assay for the impregnated biochar obtained at the process temperature of 450 °C.

Table 4 shows the EDX for the chemically modified biochar samples. There was a presence of sodium in its structure, which decreases when the biochar is produced at a temperature of 450 °C. It also verified the increase in carbon and decrease in oxygen, showing that the higher the temperature of the process, the greater the carbonization of the raw material.

Table 4. EDX analysis of impregnated biochar.

Chemical Elements	Biochar 400 °C		Biochar 450 °C	
	Mass (w%)	Atomic Mass (%)	Mass (w%)	Atomic Mass (%)
C	50.50	61.12	64.14	74.58
O	28.82	26.17	17.64	15.42
Na	19.29	12.19	13.94	8.48
K	1.39	0.52	4.28	1.52
Total	100%	100%	100%	100%

With the SEM analysis of the biochar, an aggregated amorphous solid phase consisting of microspheres and heterogeneous structures with geometry that do not present

uniformity but fragmentation is verified, showing that the plant structure was drastically altered by the carbonization process at temperatures of 400 °C and 450 °C. In fact, the temperatures generated significant changes in the morphological structure of the açai stone seed by destroying the cellular structure of the plant, composed of cellulose, lignin, and hemicellulose.

3.4. X-ray Fluorescence Spectropia

Table 5 shows the results of the constituent elements of the biochar according to the identifications and percentage quantifications of the chemical components.

Table 5. FRX analysis of biochar impregnated and in nature.

Chemical Elements	In Nature Biochar		Impregnated Biochar	
	400 °C	450 °C	400 °C	450 °C
	Conc. (%)	Conc. (%)	Conc. (%)	Conc. (%)
Mg	0.366	0.406	0.244	0.190
Si	4.624	3.897	2.854	2.305
P	4.061	3.944	6.567	7.012
S	4.173	3.701	-	-
Al	-	-	1.921	2.170
Cl	4.173	4.003	4.933	4.594
K	45.247	49.207	47.096	49.980
Ca	17.608	18.871	14.438	17.995
Mn	4.874	4.642	3.860	4.652
Fe	11.604	8.841	8.605	6.483
Na	-	-	6.741	0.997
Others	3.270	2.488	2.741	3.622
Total	100.00%	100.00%	100.00%	100.00%

Analyzing Table 5, it appears that, with the process of impregnation of NaOH in the açai seed, there is no chemical compound sulfur after the cracking process. Likewise, there is no aluminum in the process with the in natura açai seed.

The presence of a high percentage of potassium, calcium, and iron compounds is characteristic of raw materials that come from organic plant biomass, such as the one in the work in question. The appearance of sodium occurs due to the chemical impregnation that was carried out.

Comparing the data obtained for the tests carried out for the raw materials without previous treatment and with the chemical treatment, after the cracking process with the respective temperatures shown in Table 5, it showed that for most compounds, there is no significant change and it showed approximate values.

3.5. B.E.T. Analysis

Figure 7 and Table 6 show the data obtained in the B.E.T. analysis of the biochar obtained by the thermal cracking of the açai seed at temperatures of 400 °C and 450 °C produced with the raw material in nature in the batch reactor. The analysis of gas adsorption is possible to determine the distribution of pores, pore size, and surface area. The gas used was nitrogen (N₂). The N₂ capacity increased as the ratio (P/P₀) increased, showing a maximum capacity of the adsorbed amount of 1.2271 cm³/g and 1.5391 cm³/g, for temperatures of 400 °C and 450 °C, respectively. The surface area measured was 3.9871 m²/g and 4.8884 m²/g, for the lowest and highest process temperatures, respectively.

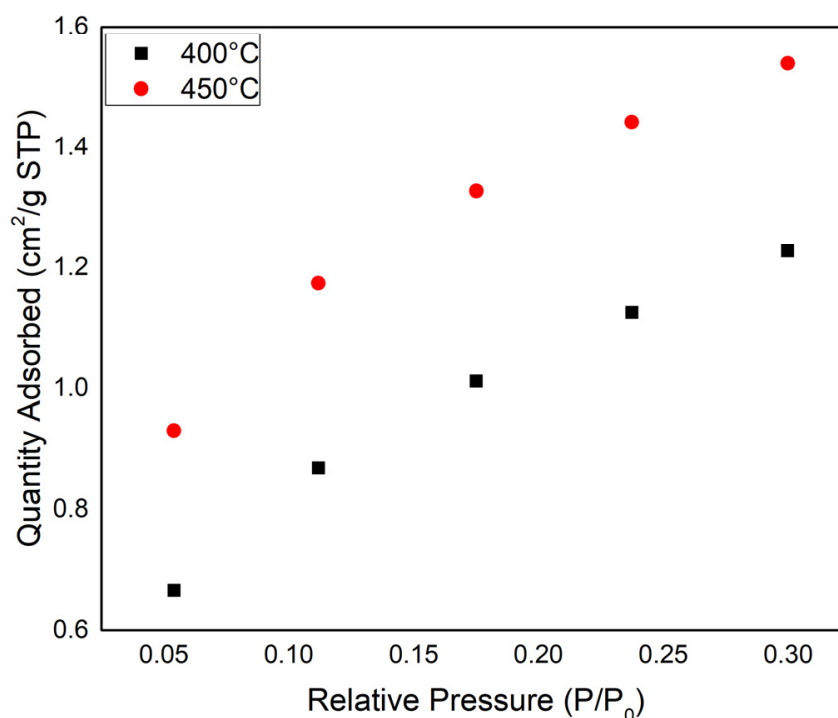


Figure 7. Adsorbed amount of N₂ by in natura biochar at 400 °C and 450 °C.

Table 6. B.E.T. analysis for the biochars obtained.

Biochar	Surface Area (m ² ·g ⁻¹)	Pore Volume (cm ³ ·g ⁻¹)	Pore Diameter (nm)	Source
400 °C	3.98	1.23	1.75	Author
450 °C	4.88	1.56	1.81	Author
400 °C (SAIN)	3.06	0.26	0.36	Castro [8]
450 °C (SAIN)	3.96	1.89	1.99	Castro [8]

As we can see in Figure 7, the adsorption process is higher at 450 °C, as we can analyze from the results that the higher the temperature, the larger the size of the pores formed. As per the IUPAC, pores with diameters or cracks with widths smaller than 2 nm are classified as micropores. Mesopores are defined as pores with a diameter between 2 and 50 nm, and macropores are those with widths or diameters greater than 50 nm. Therefore, as seen in Table 6, the pores for the two biochars are classified as micropores. The B.E.T. analyses were in agreement with the data obtained by Castro [8], in which he verified the pore size for the açai seed biochar for the temperatures of 400 °C and 450 °C, in which he obtained the surface area values of 3.06 m²/g and 3.96 m²/g for the respective temperatures. For the pore diameters, it was possible to verify an increase when compared to the temperature of 400 °C, which in the compared work was found at the value of 0.36 nm, and for the present work, the value of 1.71 nm was found.

3.6. Adsorption Equilibrium

Figures 8 and 9 below show the kinetic tests carried out using a concentration of acetic acid of 1% *v/v*, with samples of açai seed biochar in nature and impregnated, at temperatures of 400 °C and 450 °C.

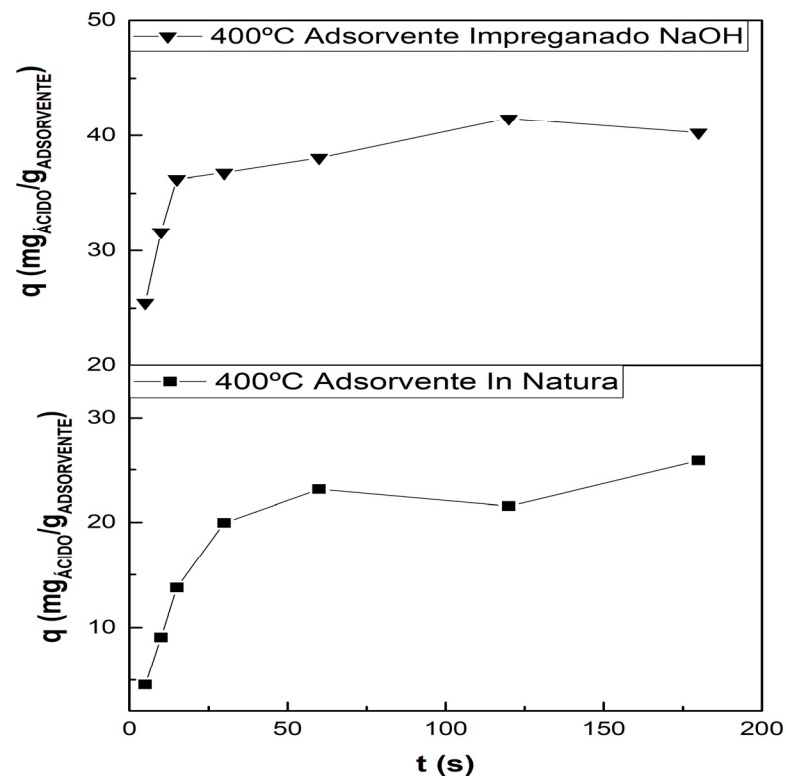


Figure 8. Equilibrium Time Chart of the kinetic assay of açai seed in nature and impregnated at a temperature of 400 °C.

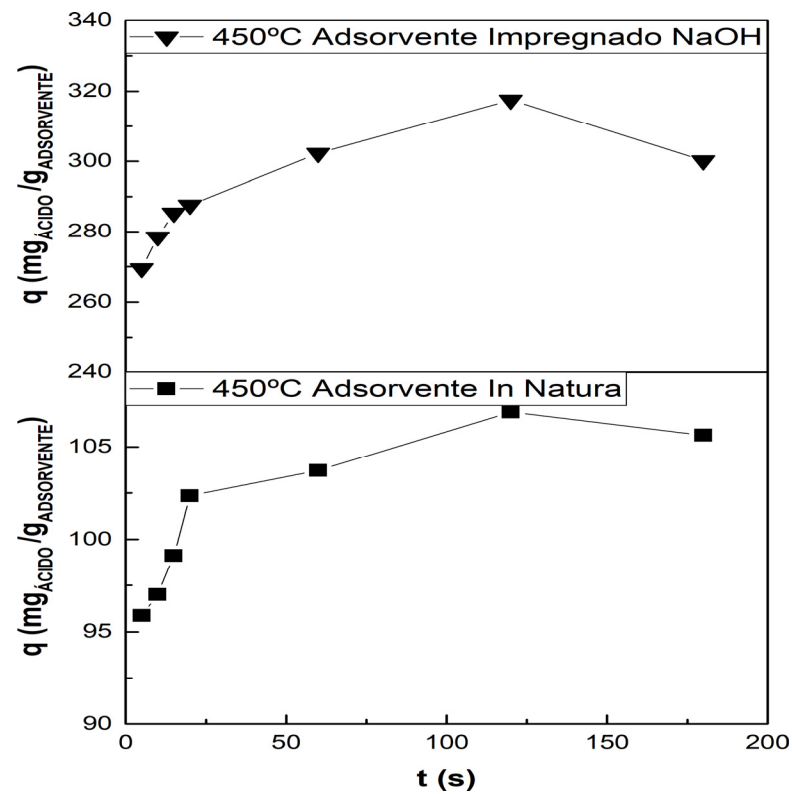


Figure 9. Equilibrium Time Chart of the kinetic assay of açai seed in nature and impregnated at a temperature of 450 °C.

The graph in Figure 8 shows the adsorption of acetic acid on in natura açai kernel charcoal impregnated with 2 M sodium hydroxide (NaOH). For this experiment, we used thermally activated carbon via thermal cracking at 400 °C. For the samples, the contact time of 180 s is shown to be sufficient to reach adsorption equilibrium.

Comparing the data for the adsorption of the in natura and impregnated açai stone charcoal, it can be seen that the material that removes the acid in a higher concentration from the solution is the charcoal impregnated with NaOH, which reached the value in 120 s of 41.50 mg_{acid}/g_{adsorbent}. After this time, acid desorption begins to occur. For the in natura charcoal, the highest adsorbed value was 25.86 mg_{acid}/g_{adsorbent}. For the time of 180 s, it was verified in the test that there was a drop in time from 60 s to 120 s, increasing again for the time of 180 s, and after that, it maintained its equilibrium, suffering desorption.

With the test carried out, it is possible to verify that the pores for the chemically impregnated coal presented a greater contact surface and, therefore, better efficiency in the adsorption process.

The graph in Figure 9 shows the adsorption test of acetic acid with açai stone charcoal in nature and chemically impregnated with NaOH at a concentration of 2 M. The material used for the adsorption process was in nature and impregnated coal, produced via thermal cracking at a temperature of 450 °C. As for the temperature of 400 °C, it was found that the contact time of 180 s was enough for the sample to reach adsorption equilibrium.

Comparing the adsorption data for the carbon material in nature and chemically impregnated, it can be seen that the chemically treated carbon presented a more efficient adsorption process, reaching a maximum value of 317.51 mg_{acid}/g_{adsorbent}, for the time of 120 s, after which an acid desorption process took place. For the in natura charcoal, the highest value was 106.87 mg_{acid}/g_{adsorbent} for a contact time of 120 s.

The result reinforces what happened at the temperature of 400 °C, showing that there is an increase in active pores for the adsorption of acids when the material undergoes a chemical treatment.

Comparing the studies, with the temperature variations of 450 °C and 400 °C, it is possible to verify the increase in the efficiency of the adsorption process with the increase in the cracking temperature. With the impregnated materials, there is a difference of 276 mg_{acid}/g_{adsorbent} more adsorbed by the material that was obtained via the thermal cracking process at a temperature of 450 °C. For the in natura materials, the difference was 81.01 mg_{acid}/g_{adsorbent} more for the material that was obtained via thermal cracking at 400 °C.

3.7. Pseudo-First-Order and Pseudo-Second-Order Kinetic Models

Figures 10 and 11 show the graphs with the adjustments of the results of the adsorption processes of acetic acid with the adsorbent of the açai seeds in nature for the temperatures of 400 °C and 450 °C for the kinetic modeling of the pseudo-first order and pseudo-second order, and Figure 10 shows the model parameters for the experiments.

The analysis of the graphs presented in Figures 10 and 11 show us that the pseudo-first-order and pseudo-second-order kinetic models are applicable to the process of the adsorption of biochar from in natura açai seeds at temperatures of 400 °C and 450 °C.

Table 7 shows the parameters obtained. It is possible to identify, as seen in the graphs of Figures 8 and 9, that the equilibrium and the adsorption capacity are greater for the experiments of biochar obtained at 450 °C, presenting in both cases greater adsorption capacity for the pseudo-second-order models. The kinetic models fit the experimental data, showing a better fit for the 450 °C experiments that presented R² of 0.99 for both models. For the temperature of 400 °C, they presented R² of 0.951 and 0.930, respectively, for the pseudo-first-order and pseudo-second-order models, showing a better fit for the first-order model.

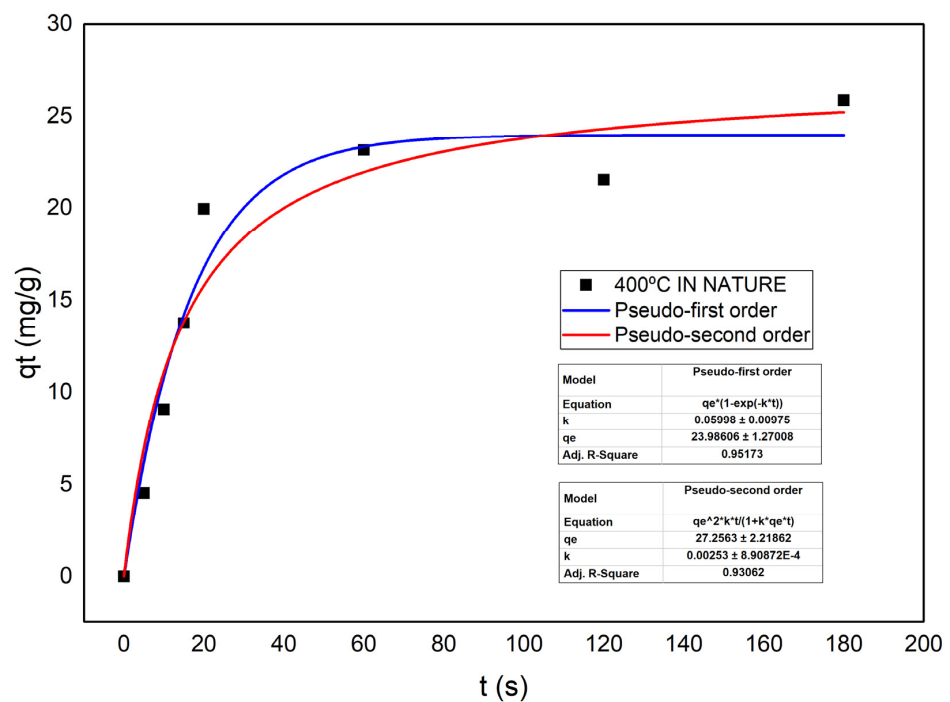


Figure 10. Pseudo-first-order and pseudo-second-order models for adsorption experiment of in nature biochar obtained at 400 °C.

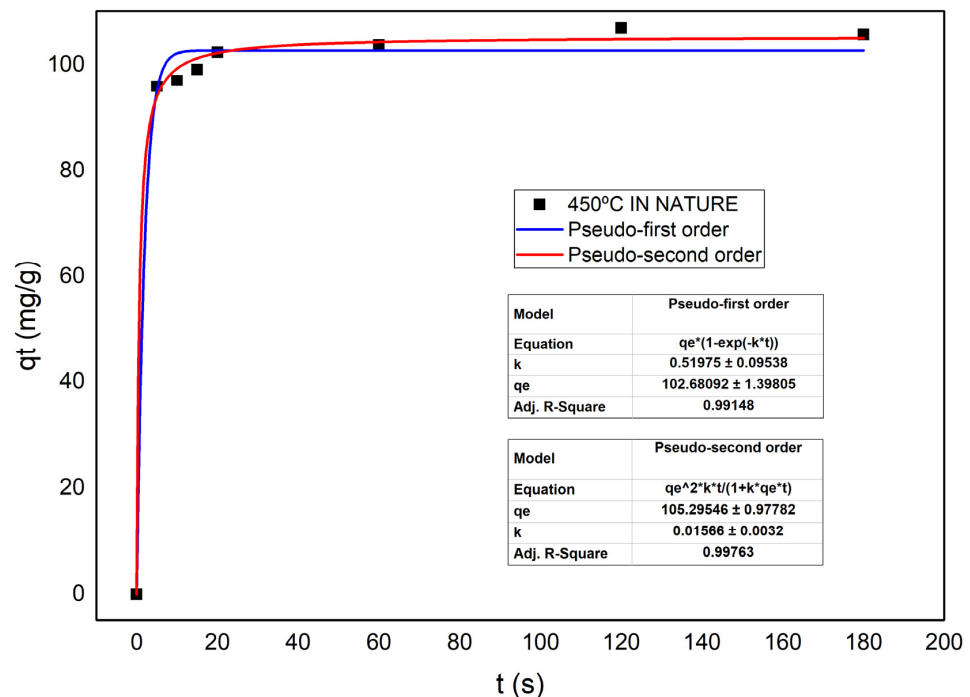


Figure 11. Pseudo-first-order and pseudo-second-order models for adsorption experiment of in nature biochar obtained at 450 °C.

Figures 12 and 13 show the graphs with the adjustments of the results of the adsorption processes of acetic acid with the adsorbent of the açai seeds impregnated at the temperatures of 400 °C and 450 °C, for the kinetic modeling of pseudo-first order and pseudo-second order, and Table 8 shows the model parameters for the experiments.

Table 7. Parameters of pseudo-first-order and pseudo-second-order kinetic models for biochar in nature.

Parameter	q _e	K	R ²
Pseudo-first Order 400 °C	23.98	0.059	0.951
Pseudo-second Order 400 °C	27.25	0.0025	0.930
Pseudo-first Order 450 °C	102.68	0.51	0.991
Pseudo-second Order 450 °C	105.29	0.015	0.997

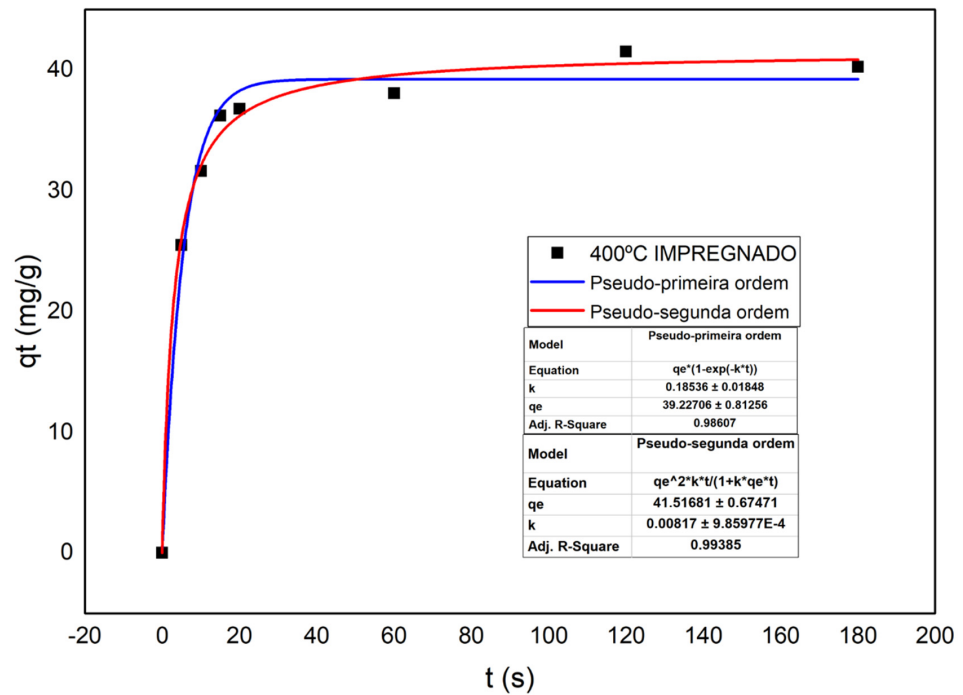


Figure 12. Pseudo-first-order and pseudo-second-order models for adsorption experiment of impregnated biochar obtained at 400 °C.

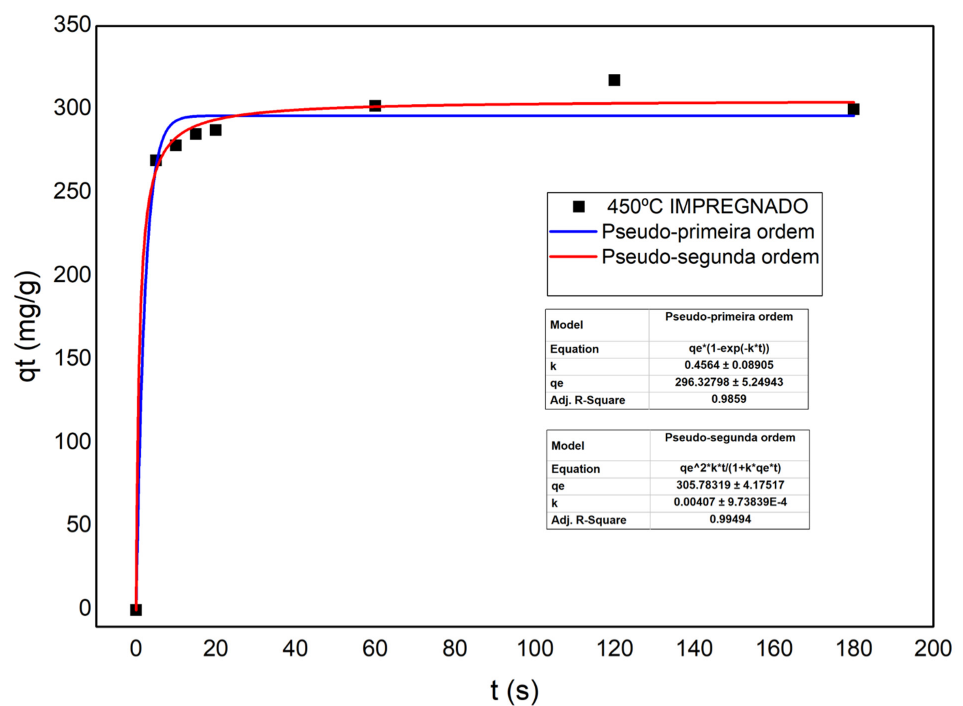


Figure 13. Pseudo-first-order and pseudo-second-order models for the adsorption experiment of impregnated biochar obtained at 450 °C.

Table 8. Parameters of pseudo-first-order and pseudo-second-order kinetic models for biochar impregnated.

Parameter	q _e	K	R ²
Pseudo-first-order 400 °C	39.22	0.185	0.986
Pseudo-second-order 400 °C	41.51	0.008	0.993
Pseudo-first-order 450 °C	296.32	0.45	0.985
Pseudo-second-order 450 °C	305.78	0.004	0.994

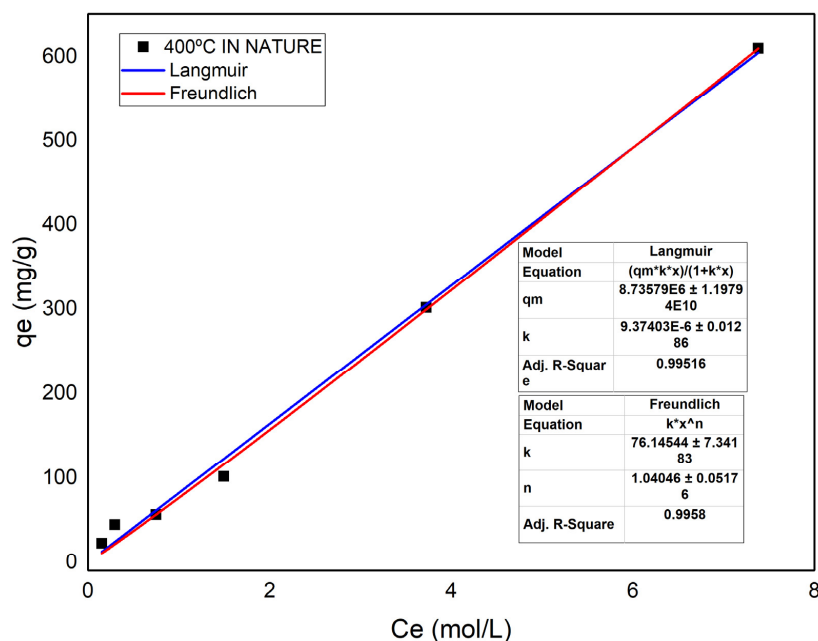
The analysis of the graphs presented in Figures 12 and 13 show us that the pseudo-first-order and pseudo-second-order kinetic models are applicable to the adsorption process of impregnated açai seed biochar at temperatures of 400 °C and 450 °C.

Table 8 shows the parameters and how much the curves were adjusted to the experimental one. It can be seen that the pseudo-first-order and pseudo-second-order models were better adjusted for the adsorption data of the impregnated açai seed, presenting an R² of 0.986 and 0.994 when compared with the data in Table 7. As it was possible to verify in the equilibrium time, the calculated adsorption capacity was higher for the experiments impregnated at a temperature of 450 °C.

3.8. Adsorption Equilibrium Isotherms of Acid Acetic (CH₃COOH) on Biochar

The Langmuir and Freundlich isotherms were applied to correlate the equilibrium adsorption data of CH₃COOH on in natura and chemically activated biochar produced by the açai seed pyrolysis process.

The adsorption isotherm of acetic acid on biochar in nature for the pyrolysis temperature of 400 °C and 450 °C was correlated with the Langmuir and Freundlich model, showing mean square errors (R²) of 0.995 and 0.995 for 400 °C and 0.995 and 0.994 at 450 °C, respectively. The equilibrium concentration in the adsorbent phase of CH₃COOH for biochar in nature at 400 °C and 450 °C was approximately 600 and 700 mg/g, respectively, as shown in Figures 14 and 15. The equilibrium loads of the bio-adsorbent (biochar) were in agreement with the adsorption of acetic acid on hydro-chars activated by NaOH and HCl produced by a hydrothermal corn husk process, as reported by Costa et al. [39], and correlated using the adsorption isotherm by the Langmuir model [39]. For the adsorption kinetics of acetic acid on the hydro-chars activated by NaOH and HCl produced by the hydrothermal corn husk process, the maximum adsorption loads of 650 mg/g and 575 mg/g were found [39], respectively.

**Figure 14.** Langmuir and Freundlich isotherm model for adsorption experiment of in natura biochar obtained at 400 °C.

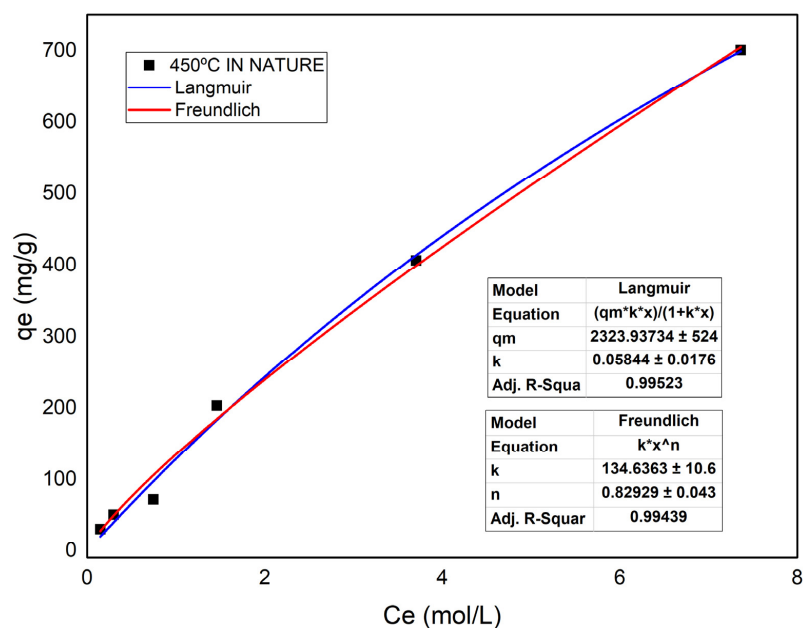


Figure 15. Langmuir and Freundlich isotherm model for adsorption experiment of in natura biochar obtained at 450 °C.

The adsorption isotherm of acetic acid on chemically activated biochar with NaOH for the pyrolysis temperature of 400 °C and 450 °C was correlated with the Langmuir and Freundlich model, presenting mean square errors (R^2) of 0.997 and 0.998 for 400 °C and 0.996 and 0.998 at 450 °C, respectively. The equilibrium concentration in the adsorbent phase of acetic acid for chemically activated biochar at 400 °C and 450 °C was approximately 800 and 3000 mg/g, respectively, as shown in Figures 16 and 17. The equilibrium charges of the biochar were above found in the adsorption of acetic acid on the hydro-chars activated by NaOH and HCl produced by the hydrothermal corn husk process, as reported by Costa et al. [39]. This shows the importance of the chemical activation process of the raw material for the production of biochar with high efficiency.

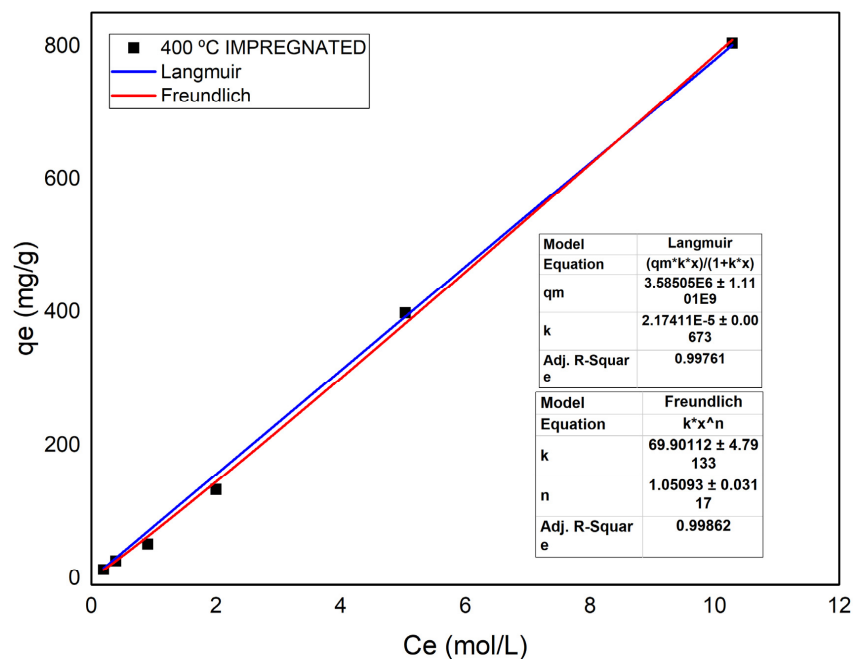


Figure 16. Langmuir and Freundlich isotherm model for adsorption experiment of chemically activated biochar obtained at 400 °C.

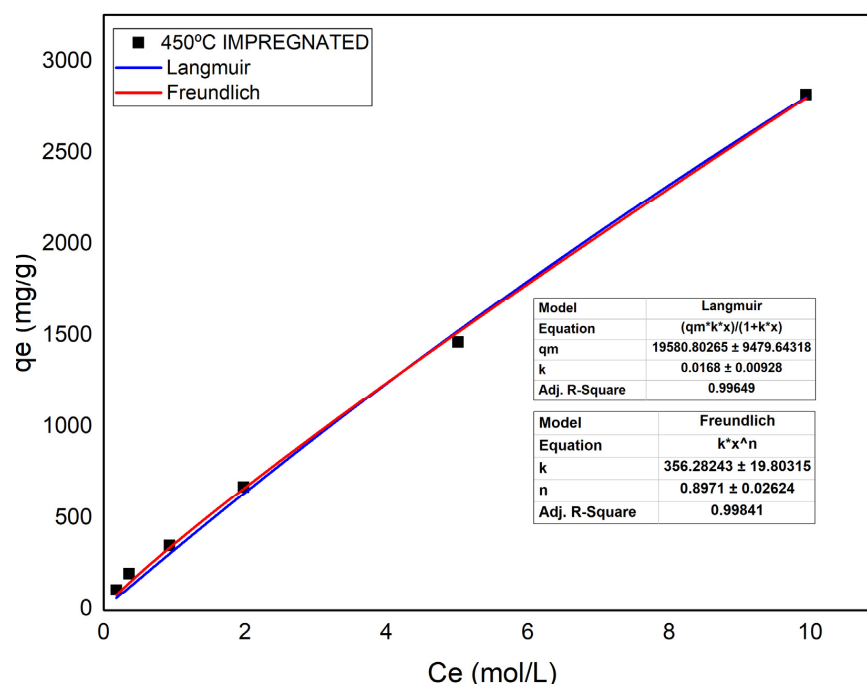


Figure 17. Langmuir and Freundlich isotherm model for adsorption experiment of chemically activated biochar obtained at 450 °C.

4. Conclusions

The SEM images of the raw material in nature showed a fibrous, rigid, and well-organized structure. Unlike the SEM images for the biochar from the açai seed in nature, which after the pyrolysis process showed better-defined pores, a greater number of pores was found for the temperature of 450 °C. For the SEM image, the impregnated açai seed presented a more open morphology with larger pores in its structure. In the semi-quantitative analysis of the EDX, it is possible to verify the increase in carbon and the reduction in oxygen for both temperatures, showing that carbonization occurs in addition to the permanence in the structure of the NaOH-impregnated biochar.

In the XRF analysis, there was a high percentage of compounds characteristic of lignocellulosic raw materials such as potassium, calcium, iron, and sodium appearing in the impregnated raw material.

In the data obtained from the B.E.T. analysis of the in natura biochar at temperatures of 400 °C and 450 °C, the maximum adsorbed capacity was higher for the biochar produced with the highest temperature, and the surface area measured was also higher for the process temperature of at 450 °C. The data obtained were in agreement with those found by Castro [8] regarding the data found for the same process temperature and the raw material for the in natura açai seed.

In the analysis of the adsorption kinetics data of acetic acid, the main carboxylic acid identified in the liquid phase showed that the biochar obtained via thermal cracking at 450 °C for the raw material impregnated with NaOH (2 M) presented greater adsorption capacity; therefore, it was possible to perceive that the activated biochars were selective in the adsorption of acetic acid, demonstrating that it is possible for the produced biochar to be applied for the removal of the free carboxylic acids present in biofuels produced via the thermal cracking of biomass and renewable materials.

Author Contributions: The individual contributions of all the co-authors are provided as follows: L.H.H.G. contributed to the methodology, formal analysis, and writing of the original draft paper; A.C.F.B. contributed to the formal analysis, methodology, and software; S.D.J. contributed to the formal analysis and software; F.P.d.C.A. contributed to the formal analysis and software; A.M.P. contributed to the formal analysis and software; G.d.O.R. contributed to the chemical analysis; R.L.e.O. contributed to the investigation, methodology, and chemical analysis; E.M.P.d.S. contributed to the resources and infrastructure; N.T.M. contributed to the resources and infrastructure; D.A.R.d.C. to the methodology, formal analysis, and co-supervision; and M.C.S. contributed to the supervision, conceptualization, and data curation. All authors have read and agreed to the published version of the manuscript.

Funding: This research received no external funding.

Institutional Review Board Statement: Not applicable.

Informed Consent Statement: Not applicable.

Data Availability Statement: Not applicable.

Conflicts of Interest: The authors declare no conflict of interest.

References

1. Liu, C.; Li, Y.; Luan, Z.; Chen, Z.; Zhang, Z.; Jia, Z. Adsorption removal of phosphate from aqueous solution by active red mud. *J. Environ. Sci.* **2007**, *19*, 1166–1170. [[CrossRef](#)]
2. Budziak, C.; Maia, C.M.B.F.; Mangrich, A.S. Transformações químicas da matéria orgânica durante a compostagem de resíduos da indústria madeireira. *Química Nova* **2004**, *27*, 399–403. [[CrossRef](#)]
3. Gurgel, L.V.A. Mercerização e Modificação Química de Celulose e Bagaço de Cana-de-açúcar Com Anidrido Succínico e Trietilenotetramina: Preparação de novos Materiais Quelantes para a Adsorção de Pb (II), Cd (II), Cr (VI) e Cu (II). Master's Thesis, Universidade Federal de Ouro Preto, Ouro Preto, Brazil, 2007.
4. Canettieri, E.V. Obtenção dos Parâmetros e Estudo Cinético da Hidrólise Ácida dos Resíduos Florestais de Eucalipto. Ph.D. Thesis, Faculdade de Engenharia de Guaratinguetá, Universidade Estadual Paulista, Guaratinguetá, Brazil, 2004.
5. Huber, G.W.; Dumesic, J.A. An overview of aqueous-phase catalytic processes for production of hydrogen and alkanes in a biorefinery. *Catal. Today* **2006**, *111*, 119–132. [[CrossRef](#)]
6. Li, J.; Yu, G.; Xie, S.; Pan, L.; Li, C.; You, F.; Wang, Y. Immobilization of heavy metals in ceramsite produced from sewage sludge biochar. *Sci. Total Environ.* **2018**, *628–629*, 131–140. [[CrossRef](#)] [[PubMed](#)]
7. Oliveira, M.S.P.; Carvalho, J.E.U.; Nascimento, W.M.O. *Açaí (Euterpe oleracea Mart.)*; Funep: Jaboticabal, Brazil, 2000.
8. de CASTRO, D.A.R. Estudo do Processo de Pirólise de Sementes de AÇAÍ (Euterpe oleracea Mart.) para Produção de Biocombustíveis. Ph.D. Thesis, Curso de Engenharia de Recursos Naturais da Amazônia, ITEC, Universidade Federal do Pará, Belém, Brazil, 2019.
9. Liu, T.; Liu, B.; Zhang, W. Nutrients and heavy metals in biochar produced by sewage sludge pyrolysis: Its application in soil amendment. *Pol. J. Environ. Stud.* **2014**, *23*, 271–275.
10. Ahmad, M.; Lee, S.S.; Dou, X.; Mohan, D.; Sung, J.K.; Yang, J.E.; Ok, Y.S. Effects of pyrolysis temperature on soybean stover- and peanut shell-derived biochar properties and TCE adsorption in water. *Bioresour. Technol.* **2012**, *118*, 536–544. [[CrossRef](#)]
11. Zielińska, A.; Oleszczuk, P. Evaluation of sewage sludge and slow pyrolyzed sewage sludge-derived biochar for adsorption of phenanthrene and pyrene. *Bioresour. Technol.* **2015**, *192*, 618–626. [[CrossRef](#)]
12. Chandra, R.; Takeuchi, H.; Hasegawa, T. Hydrothermal pretreatment of rice straw biomass: A potential and promising method for enhanced methane production. *Appl. Energy* **2012**, *94*, 129–140. [[CrossRef](#)]
13. da COSTA, K.M.B. Desacidificação de Frações Destiladas de Produto Líquido Orgânico do Craqueamento Termo-Catalítico de Óleos Vegetais Via Adsorção em γ -Alumina e Lama Vermelha Ativada. Master's Thesis, Universidade Federal do Pará, Belém, Brazil, 2015.
14. Rodríguez-Zúñiga, U.; Lemo, V.; Farinas, C.; Bertucci Neto, V.; Couri, S. Evaluation of agroindustrial residues as substrates for cellulolytic enzymes production under solid state fermentation. In *7SBPMat, 2008, Guarujá; Brazilian MRS Meeting; SBPMat: Rio de Janeiro, Brazil, 2008*.
15. Carrier, M.; Loppinet-Serani, A.; Denux, D.; Lasnier, J.-M.; Ham-Pichavant, F.; Cansell, F.; Aymonier, C. Thermogravimetric analysis as a new method to determine the lignocellulosic composition of biomass. *Biomass Bioenergy* **2011**, *35*, 298–307. [[CrossRef](#)]
16. Sorek, N.; Yeats, T.H.; Szemenyei, H.; Youngs, H.; Somerville, C.R. The Implications of Lignocellulosic Biomass Chemical Composition for the Production of Advanced Biofuels. *BioScience* **2014**, *64*, 192–201. [[CrossRef](#)]
17. Acharjee, T.C.; Coronella, C.J.; Vasquez, V.R. Effect of thermal pretreatment on equilibrium moisture content of lignocellulosic biomass. *Bioresour. Technol.* **2011**, *102*, 4849–4854.
18. Irfan, M.; Chen, Q.; Yue, Y.; Pang, R.; Lin, Q.; Zhao, X.; Chen, H. Co-production of biochar, bio-oil and syngas from halophyte grass (*Achnatherum splendens* L.) under three different pyrolysis temperatures. *Bioresour. Technol.* **2016**, *211*, 457–463. [[CrossRef](#)]

19. Cordeiro, M.A. Estudo da Hidrólise Enzimática do Caroço de Açaí (Euterpe oleracea Mart) para a Produção de Etanol. Programa de Pós-Graduação em Engenharia Química, UFPA. Master's Thesis, Federal University of Pará, Belém, Brazil, 2016.
20. Rangel, R. Modelagem, caracterização e simulação da pirólise do semente de açaí. 74 f. Trabalho de Conclusão do Curso. Bachelor's Thesis, Graduação em Engenharia de Energia, Universidade de Brasília, Brasília, Brazil, 2015.
21. Spence, K.L.; Venditti, R.A.; Habibi, Y.; Rojas, O.J.; Pawlak, J.J. The effect of chemical composition on microfibrillar cellulose films from wood pulps: Mechanical processing and physical properties. *Bioresour. Technol.* **2010**, *101*, 5961–5968. [[CrossRef](#)]
22. Huang, J.; Liu, C.; Tong, H.; Li, W.; Wu, D. Theoretical studies on pyrolysis mechanism of xylopyranose. *Comput. Theor. Chem.* **2012**, *1001*, 44–50. [[CrossRef](#)]
23. Pauly, M.; Gille, S.; Liu, L.; Mansoori, N.; de Souza, A.; Schultink, A.; Xiong, G. Hemicellulose biosynthesis. *Planta* **2013**, *238*, 627–642.
24. Laird, D.A. The Charcoal Vision: A Win-Win-Win Scenario for Simultaneously Producing Bioenergy, Permanently Sequestering Carbon, while Improving Soil and Water Quality. *Agron. J.* **2008**, *100*, 178. [[CrossRef](#)]
25. Nakagawa, K.; Namba, A.; Mukai, S.R.; Tamon, H.; Ariyadejwanich, P. Adsorption of phenol and reactive dye from aqueous solution on activated carbons derived from solid wastes. *Water Res.* **2004**, *38*, 1791–1798. [[CrossRef](#)]
26. Chen, W.; Parette, R.; Zou, J.; Cannon, F.S.; Dempsey, B.A. Arsenic removal by iron-modified activated carbon. *Water. Res.* **2007**, *41*, 1851–1858. [[CrossRef](#)]
27. Sato, M.K.; Lima, H.V.; Costa, A.N.; Rodrigues, S.; Mooney, S.J.; Clarke, M.; Pedroso, A.J.S.; Maia, C.M.B.F. Biochar as sustainable alternative to açai waste disposal in Amazon, Brazil. *Process Saf. Environ. Prot.* **2020**, *139*, 36–46. [[CrossRef](#)]
28. Ruthven, D.M. *Principles of Adsorption and Adsorption Process*; John Wiley & Sons: New York, NY, USA, 1984.
29. van de Velden, M.; Baeyens, J.; Brems, A.; Janssens, B.; Dewil, R. Fundamentals, kinetics and endothermicity of the biomass pyrolysis reaction. *Renew. Energy* **2010**, *35*, 232–242. [[CrossRef](#)]
30. Faccini, C.S.; Cunha, M.E.d.; Moraes, M.S.A.; Krause, L.C.; Manique, M.C.; Rodrigues, M.R.A.; Benvenutti, E.V.; Caramão, E.B. Dry washing in biodiesel purification: A comparative study of adsorbents. *J. Braz. Chem. Soc.* **2011**, *22*, 558–563. [[CrossRef](#)]
31. Manuale, D.L.; Mazzieri, V.A.; Torres, G.; Vera, C.R.; Yori, J.C. Non catalytic biodiesel process with adsorption-based refining. *Fuel* **2011**, *90*, 1188–1196. [[CrossRef](#)]
32. Guimarães de Mello, M. *Energia da Biomassa—A grande oportunidade de Minas e do Brasil*; Cemig: Belo Horizonte, Brazil, 2001; p. 21.
33. Suzuki, M. *Adsorption Engineering*; Kodansha: Tokyo, Japan, 1990.
34. Franca, A.S.; Oliveira, L.S.; Nunes, A.A.; Alves, C.C.O. Microwave assisted thermal treatment of defective coffee beans press cake for the production of adsorbents. *Bioresour. Technol.* **2010**, *101*, 1068–1074. [[CrossRef](#)]
35. Rambo, M.K.D. Caracterização de Resíduos Lignocelulósicos por Espectroscopia NIR Aliada à Quimiometria para a Obtenção de Insumos Químicos. Ph.D. Thesis, Universidade Estadual de Campinas, Instituto de Química, Campinas, SP, Brazil, 2013.
36. Seye, O.; Souza, R.C.R.; Bacellar, A.A.; Morais, M.R. Caracterização do caroço de açaí como insumo para geração de eletricidade via gaseificação. In Proceedings of the Congresso Internacional Sobre Geração Distribuída E Energia No Meio Rural, Fortaleza, Brazil, 23–26 September 2008.
37. Silva, L.G.; Neto, A.M.J.C.; Gaffo, L.; Borges, R.S.; Ramalho, T.; Machado, N. Molecular Dynamics of Film Formation of Metal Tetrasulfonated Phthalocyanine and Poly Amidoamine Dendrimers. *J. Nanomater.* **2013**, *2013*, 816285. [[CrossRef](#)]
38. Leão, R.M. Tratamento Superficial de Fibra de Coco e Aplicação em Materiais Compósitos Como Reforço do Polipropileno. Master's Thesis, Engenharia Mecânica, Universidade de Brasília, Brasília, Brazil, 2012.
39. Costa, M.E.G.; da Costa Assunção, F.P.; Teribele, T.; Pereira, L.M.; de Castro, D.A.R.; Santos, M.C.; da Costa, C.E.F.; Shultze, M.; Hofman, T.; Machado, N.T. Characterization of Bio-Adsorbents Produced by Hydrothermal Carbonization of Corn Stover: Application on the Adsorption of Acetic Acid from Aqueous Solutions. *Energies* **2021**, *14*, 8154. [[CrossRef](#)]